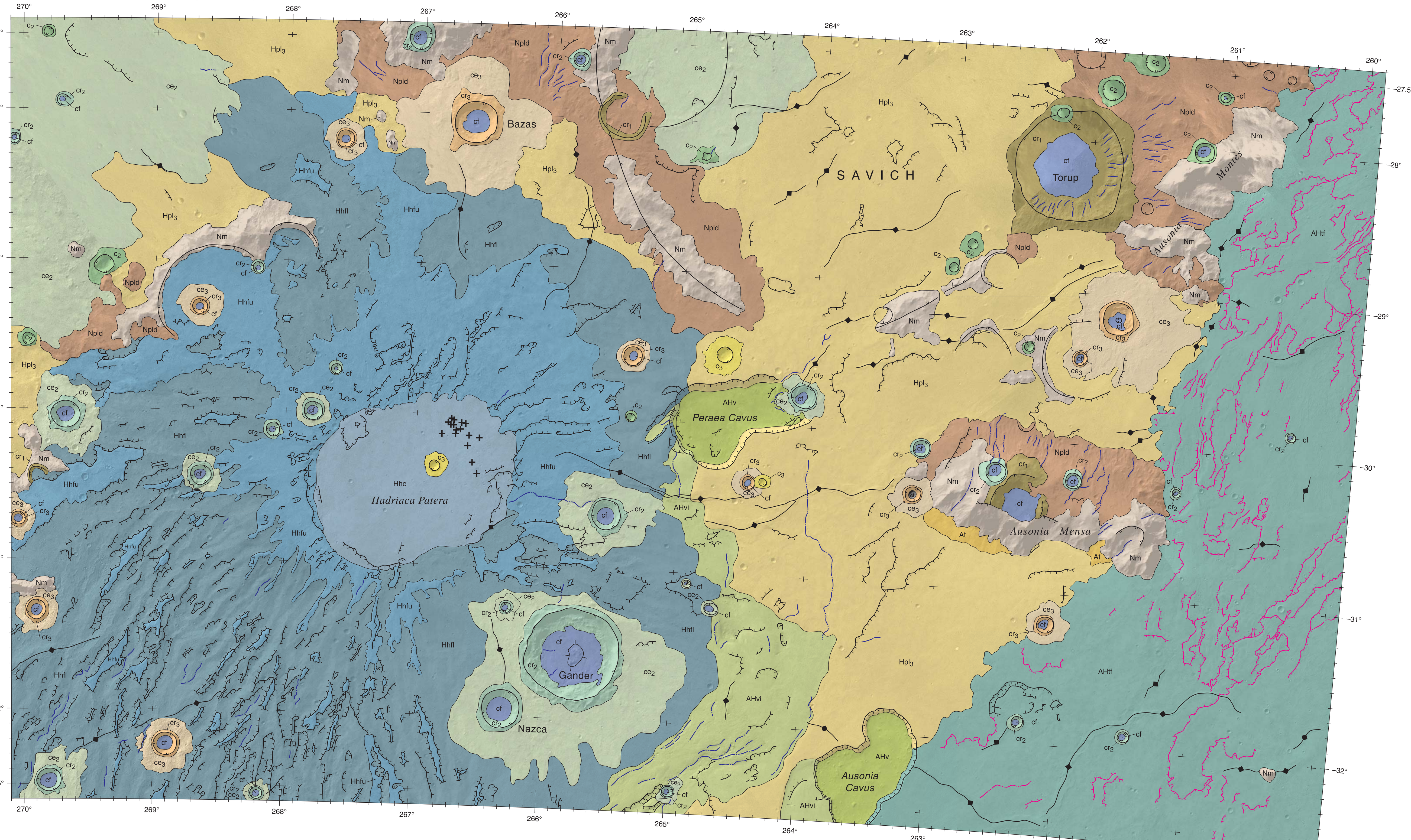

Descriptions of nomenclature used on map are listed at http://planetarynames.wr.usgs.gov/

SCALE 1:1 004 000 (1 mm = 1.004 km) AT 270° LONGITUDE
TRANSVERSE MERCATOR PROJECTION
20 0 20 40 60 80 100
KILOMETERS
Planetographic latitude and west longitude coordinate system

Prepared on behalf of the Planetary Geology and Geophysics Program, Solar System Exploration Division, Office of Space Science, National Aeronautics and Space Administration
Edited by Jan L. Zigler; cartography by Darlene A. Ryan
Manuscript approved for publication July 17, 2006

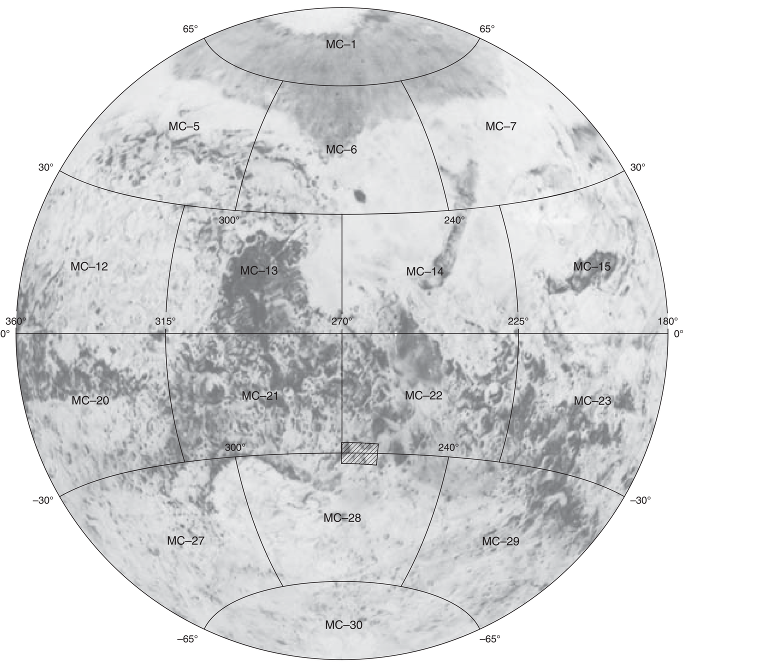

QUADRANGLE LOCATION

Photomosaic showing location of map area. An outline of 1:5,000,000-scale quadrangles is provided for reference.

Table 1. *Crater size-frequency data and relative age determinations for geologic units in the Hadriaca Patera region of Mars.*

[Data from regional study (Crown and others, 1992) of MTM –30262, –30267, –30272, –35262, –35267, –35272, -40262, –40267, and –40272 quadrangles; total number of craters and area represent entire unit exposures within these nine quadrangles. N(2), N(5), and N(16) are cumulative number of craters >2, >5, and >16 km in diameter per 10^6 km^2; error = $\pm [(n(x)^{1/2})/A] \times 10^6$, where n = number of craters > x km in diameter and A = area. Age range is based on superposition relations and crater counts using the crater-density boundaries of Tanaka (1986): EA, Early Amazonian; LH, Late Hesperian; EH, Early Hesperian; LN, Late Noachian; MN, Middle Noachian]

Unit label	Total no. craters	Area (km2)	N(2)	N(5)	N(16)	Age range (epoch)
AHvt[1]	56	45,947	239±72	109±49	0	EA–LH
Hhc	10	5,744	174±174	0	0	LH or younger
AHtf	188	80,576	397±70	87±33	0	EA–LH
Hhft[2]	349	103,089	572±75	175±41	19±14	EH
Hpl$_3$	366	121,447	519±65	165±37	33±17	EH
Npld	80	24,210	1,070±211	413±131	123±72	LN–MN
Nm	74	35,101	826±153	285±90	86±49	LN–MN

[1]Unit AHvt includes vallis floor material (AHv) and irregular vallis floor material (AHvi).
[2]Unit Hhft includes Hadriaca Patera upper (Hhfu) and lower flank (Hhfl) materials.

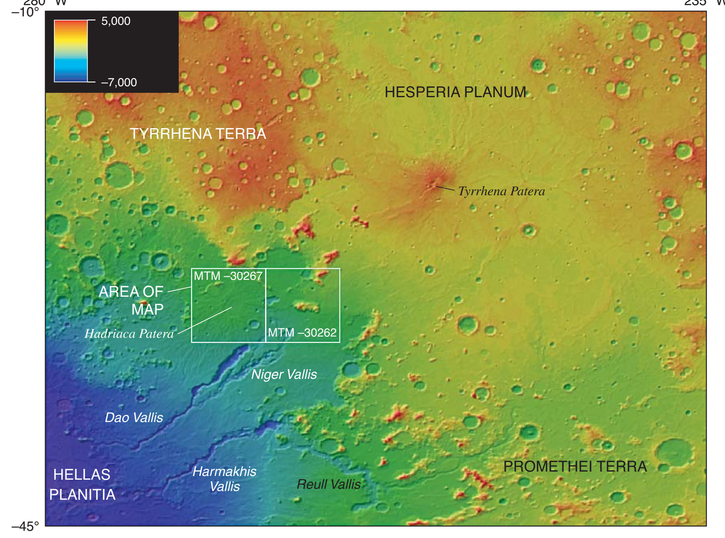

Figure 1. MOLA DEM (128 pixels/degree) of northeastern Hellas Planitia and Hesperia Planum, Mars, showing map area (MTM –30262 and –30267 quadrangles). Locations of highland paterae, canyon systems, and major physiographic provinces are indicated.

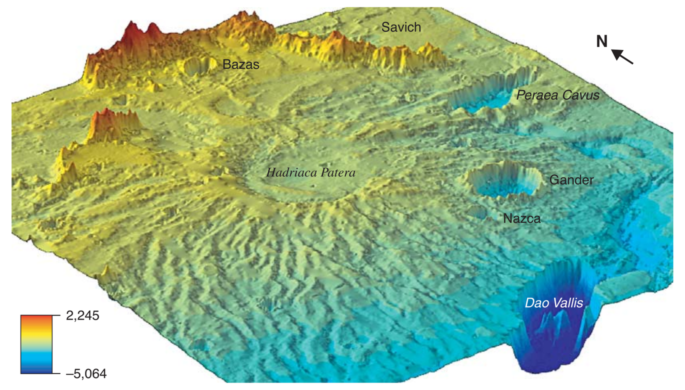

Figure 2. Perspective view of MOLA DEM (128 pixels/degree) of summit region of Hadriaca Patera, showing low relief of volcano, dissected patera flanks, and topographic depressions associated with parts of Dao and Niger Valles systems (fig. 1). Northwest of ~77 km-diameter caldera, patera flanks slope slightly uphill and appear to be confined by remnant of rugged crater rim. View to northeast; vertical exaggeration x 10.

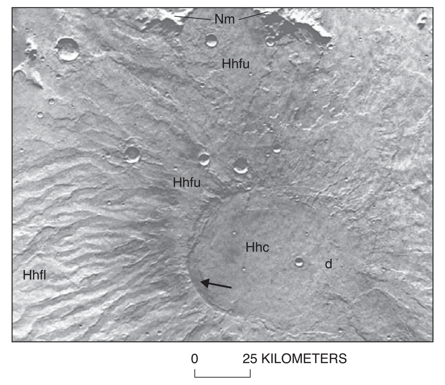

Figure 3. Viking Orbiter image (410S02, 166 m/pixel resolution) of summit caldera of Hadriaca Patera. The morphology of the west rim is indicative of collapse; to the north and east, the rim may be covered by volcanic materials. Small dome-like features (d) are observed on the surface of Hadriaca Patera caldera-filling material (unit Hhc) in the eastern part of the caldera. Erosional scarps are apparent; some incise the caldera rim. A large scarp (arrow) in the southwest may be the margin of ponded lavas. Hadriaca Patera lower flank material (unit Hhfl) is visible south and west of the caldera. A plateau of Hadriaca Patera upper flank material (unit Hhfu) surrounds the caldera to the west and north. North is toward the upper right.

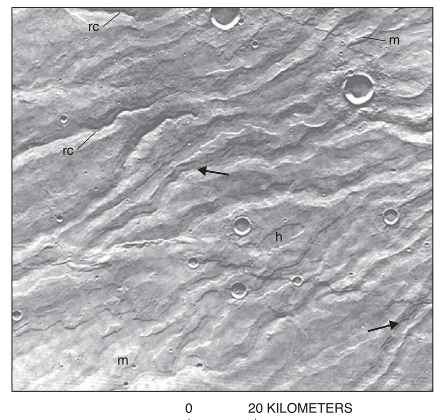

Figure 5. Viking Orbiter image (408S67, 108 m/pixel resolution) of the channeled flanks of Hadriaca Patera. The channels are trough-shaped valleys extending radially from the summit caldera. Layers are exposed in channel walls (arrows). Note theater-headed valleys indicative of groundwater sapping (h) and V-shaped runoff channels (rc) in the centers of some valleys. Erosional remnant mesas (m) are evident within Hadriaca Patera lower flank material (unit Hhfl). North is toward the upper right.

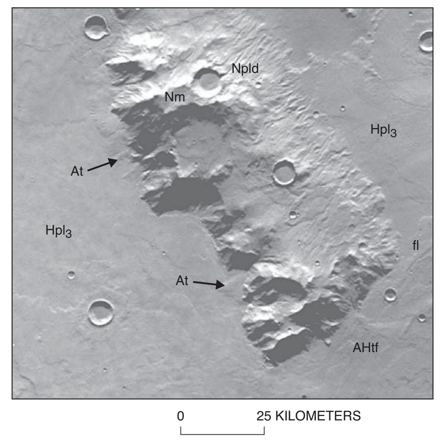

Figure 4 (left). Viking Orbiter image (411S02, 103 m/pixel resolution) showing an isolated massif (Ausonia Mensa) to the east of Hadriaca Patera that consists of a combination of mountainous material (unit Nm) and the dissected unit of the plateau sequence (unit Npld). On the north side, numerous parallel channels form on relatively shallow slopes, presumably by a combination of mass-wasting and fluvial processes. On the steeper south side, talus material (unit At, arrows) covers the contact between the mountainous material (unit Nm) and the surrounding plains (unit Hpl$_3$). Part of a discontinuous leveed channel is observed at the center of a flow lobe (fl) in the Tyrrhena Patera flank flow unit (unit AHtf), whose flows superpose unit Hpl$_3$ at the bottom center of the image. Ausonia Mensa and the surrounding plains exhibit a series of medium-sized craters with a range of degradation states (see crater materials in Description of Map Units). North is toward the upper right.

CORRELATION OF MAP UNITS

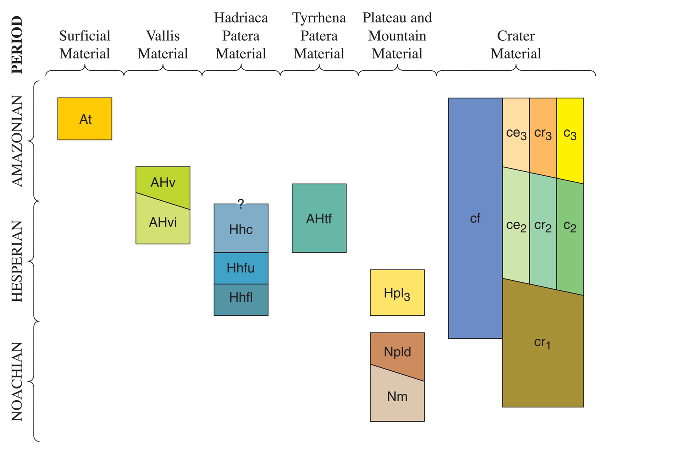

DESCRIPTION OF MAP UNITS

SURFICIAL MATERIAL

At **Talus material (Middle Amazonian or younger)**—Deposits border mountainous material (unit Nm) of Ausonia Mensa and extend as far as ~10 km from them. Occurs where mountainous material is steep. Some linear features observed at margins of unit. *Interpretation*: Debris shed from steep blocks of uplifted crust. Linear features may indicate fluvial or mass-wasting processes

VALLIS MATERIAL

AHv **Vallis floor material (Early Amazonian to Late Hesperian)**—Smooth material, containing isolated blocks 0.5–2 km across, forms floors of depressions bordered by steep scarps. *Interpretation*: Sedimentary deposits forming floors of collapse depressions in water- or ice-rich materials

AHvi **Irregular vallis floor material (Early Amazonian to Late Hesperian)**—Commonly low lying deposits have smooth, low-relief surfaces dissected by small (~0.5–2.5 km wide) channels and troughs. *Interpretation*: Sedimentary and volcanic deposits (units AHtf, Hhfl, Hpl$_3$) modified by fluvial erosion in initial stages of dissection and collapse

HADRIACA PATERA MATERIAL

Hhc **Hadriaca Patera caldera-filling material (Late Hesperian or younger)**—Smooth, relatively featureless deposits partly fill depression at summit of Hadriaca Patera and have well-defined boundary at west margin. Scarps occur along margins of unit and extend into surrounding materials. *Interpretation*: Volcanic materials (lava flows or pyroclastic deposits) filling Hadriaca Patera caldera. Some scarps may represent flow margins. Unit contained within caldera to west and may overflow caldera to north and east. Unit represents late-stage volcanic activity at Hadriaca Patera

Hhfu **Hadriaca Patera upper flank material (Early Hesperian)**—Material exhibiting relatively smooth surface surrounding caldera-filling material (unit Hhc) at Hadriaca Patera. Bordered by scarps. Several layers exposed to northwest. Material is relatively continuous to north and extends more than 100 km from caldera margin; to southwest, unit consists of topographically high remnants forming ridges within Hadriaca Patera lower flank material (unit Hhfl). *Interpretation*: Volcanic deposits (probably pyroclastic flows) erupted from caldera at Hadriaca Patera and later dissected by fluvial processes. Erosional morphology indicated by presence of layering and scarps. Morphologic differences between upper and lower flank materials attributed to changes in topography and position relative to caldera and to resulting changes in degree of erosion

Hhfl **Hadriaca Patera lower flank material (Early Hesperian)**—Layered, dissected material surrounding caldera-filling material (unit Hhc) and upper flank material (unit Hhfu) at Hadriaca Patera. Pattern of dissection radial to caldera. Numerous scarps; some channels and ridges. Spacing between ridges is smaller and more layers are exposed to south and west than to north and east of caldera. *Interpretation*: Volcanic deposits (probably pyroclastic flows) erupted from caldera and later dissected by fluvial processes. Erosional morphology indicated by layering and remnant mesas. Decreased spacing of scarps reflects greater slope and resulting change in degree of erosion

TYRRHENA PATERA MATERIAL

AHtf **Tyrrhena Patera flank flow material (Early Amazonian to Late Hesperian)**—Forms deposits with rough surface containing lobate scarps and channels bounded by levees. Lobes elongated to southwest. Unit extends from Tyrrhena Patera (northeast of map area) for over 1,000 km to southwest. Some ridges observed. Embays mountainous material (unit Nm) and dissected unit of the plateau sequence (unit Npld) along its west margin in MTM –30262 and covers smooth unit of the plateau sequence (unit Hpl$_3$) near Ausonia Mensa and Ausonia Montes. *Interpretation*: Lava flows displaying lobate margins, lava channels, and possibly partially collapsed lava tubes form extensive lava flow field associated with Tyrrhena Patera. Some ridges may be associated with flow emplacement and may be partially volcanic

PLATEAU AND MOUNTAIN MATERIAL

Hpl$_3$ **Smooth unit of the plateau sequence (Early Hesperian)**—Forms flat, relatively featureless plains that fill basins and locally embay dissected unit of the plateau sequence (unit Npld) and mountainous material (unit Nm). Some ridges and scarps observed. *Interpretation*: Sedimentary deposits and volcanic materials that fill depressions and cover underlying rocks

Npld **Dissected unit of the plateau sequence (Late to Middle Noachian)**—Forms cratered surfaces of moderate to high relief with some relatively smooth areas; dissected by small channels and troughs. *Interpretation*: Materials formed during interval of intense cratering. Probably composed of impact breccia and volcanic and erosional deposits, modified by fluvial and mass-wasting processes

Nm **Mountainous material (Late to Middle Noachian)**—Forms large, rugged, isolated blocks. Also occurs as remnants of large crater rims. Scattered, smaller, less-rugged deposits surrounded by smooth plateau unit (unit Hpl$_3$). May have channels extending downslope to margin of unit. *Interpretation*: Ancient crustal material uplifted during period of heavy impact cratering. May include remnants of large crater rims. Channeling on slopes indicates modification by mass-wasting or fluvial processes

CRATER MATERIAL

[Craters and their associated rim and ejecta materials are assigned to three classes based upon their state of degradation and stratigraphic relations. Craters having rim crest diameters ≥3 km across are shown on the map. Crater materials are subdivided where floor, rim, and ejecta materials can be identified.]

cf **Crater floor material (Late Amazonian to Late Noachian)**—Forms typically smooth, featureless surfaces in crater interiors; in places, may exhibit scarps or channels. *Interpretation*: Sedimentary deposits of mass-wasting and aeolian origin that accumulate on crater floors; contributions of fluvial, glacial, and lacustrine sediments also possible

c$_3$ **Well-preserved crater material (Late to Early Amazonian)**—Pronounced, continuous crater rim that rises above surrounding materials has steep inner wall and generally well defined, continuous ejecta deposit. Crater floors are typically smooth and featureless and, in places, may exhibit scarps or channels. *Interpretation*: Youngest crater materials with minimal degradation. Crater floor may be covered by sedimentary deposits (unit cf) that are, in places, dissected by channels or faults

ce$_3$ **Ejecta material**—Generally well defined, continuous deposits surrounding crater rim material (unit cr$_3$). Example at Bazas crater north of Hadriaca Patera

cr$_3$ **Rim material**—Continuous deposits encircling and rising above crater floor, including crater wall inside rim crest. Example at Bazas crater north of Hadriaca Patera

c$_2$ **Moderately degraded crater material (Early Amazonian to Early Hesperian)**—Crater rim may exhibit only minor relief above surrounding materials. Ejecta deposits absent or discontinuous and poorly exposed; crater floors typically smooth and featureless; in places, may exhibit scarps or channels. *Interpretation*: Crater materials of moderate age and degradation state. Rim is partially eroded; ejecta may be completely eroded; crater floor may be covered by sedimentary deposits (unit cf). In places, dissected by channels or faults

ce$_2$ **Ejecta material**—Discontinuous or poorly exposed deposits that are adjacent to crater rim material (unit cr$_2$); large exposure in northwest corner of MTM –30267 is ejecta blanket from crater Isil, an ~80-km-diameter crater partly located in MTM –30272 and MTM –25272 northwest of map area. Examples at Gander and Nazca craters on southeast flanks of Hadriaca Patera

cr$_2$ **Rim material**—Continuous to discontinuous deposits encircling and, in places, rising above crater floor, including crater wall inside rim crest. Examples at Gander and Nazca craters on southeast flanks of Hadriaca Patera

Highly degraded crater material—Crater rim subdued or discontinuous and generally does not exhibit external relief; ejecta deposits not observed. Inner crater wall may exhibit scarps and channels; crater floors typically smooth and featureless but, in places, may exhibit scarps or channels. *Interpretation*: Oldest, most degraded crater materials. Ejecta is completely eroded; rim trace may be evident but rim nearly eroded to level of surrounding materials; crater floor may be covered by sedimentary deposits (unit cf), in places dissected by channels or faults

cr$_1$ **Rim material (Early Hesperian to Middle Noachian)**—Generally subdued, discontinuous deposits adjacent to crater floor material exhibiting little or no relief. Includes crater wall inside rim crest. May exhibit scarps or channels. Example at Torup crater adjacent to Ausonia Montes

Contact—Dashed where approximately located

Ridge crest

Scarp—Hachures point downscarp

Channel

Volcanic channel

Margin of volcanic flow—Hachures point downslope

Small dome or hill

Crater rim crest

Crater central peak—Hachures point downslope

Closed depression

INTRODUCTION

Mars Transverse Mercator (MTM) –30262 and –30267 quadrangles cover the summit region and east margin of Hadriaca Patera, one of the Martian volcanoes designated highland paterae (Plescia and Saunders, 1979). MTM –30262 quadrangle includes volcanic deposits from Hadriaca Patera and Tyrrhena Patera (summit northeast of map area) and floor deposits associated with the Dao and Niger Valles canyon systems (south of map area; figs. 1, 2). MTM –30267 quadrangle is centered on the caldera of Hadriaca Patera (fig. 3). The highland paterae are among the oldest, central-vent volcanoes on Mars (Scott and Carr, 1978) and exhibit evidence for explosive eruptions, which make a detailed study of their geology an important component in understanding the evolution of Martian volcanism. Photogeologic mapping at 1:500,000 scale from analysis of Viking Orbiter images complements volcanological studies of Hadriaca Patera, geologic investigations of the other highland paterae, and an analysis of the styles and evolution of volcanic activity east of Hellas Planitia in the ancient, cratered highlands of Mars (Greeley and Crown, 1990; Crown and Greeley, 1993). This photogeologic study is an extension of regional geologic mapping east of Hellas Planitia (Crown and others, 1992; Mest and Crown, 2001).

The Martian highland paterae are low-relief, areally extensive volcanoes exhibiting central calderas and radial channels and ridges (Plescia and Saunders, 1979; Greeley and Spudis, 1981). Four of these volcanoes, Hadriaca, Tyrrhena, Amphitrites, and Peneus Paterae, are located in the ancient cratered terrains surrounding Hellas Planitia and are thought to be located on inferred impact basin rings or related fractures (Peterson, 1978; Schultz, 1984). Based on analyses of Mariner 9 images, Potter (1976), Peterson (1977), and King (1978) suggested that the highland paterae were shield volcanoes formed by eruptions of fluid lavas. Later studies noted morphologic similarities between the paterae and terrestrial ash shields (Peterson, 1978; Francis and Wood, 1982) and the lack of primary lava flow features on the flanks of the volcanoes (Greeley and Crown, 1990; Crown and Greeley, 1993). The degraded appearances of Hadriaca and Tyrrhena Paterae and the apparently easily eroded materials composing their low, broad shields (Greeley and Spudis, 1981; Crown and Greeley, 1993) further suggest that the highland paterae are composed predominantly of pyroclastic deposits. Analyses of eruption and flow processes indicate that the distribution of units at Hadriaca and Tyrrhena Paterae is consistent with emplacement by gravity-driven pyroclastic flows (Crown and others, 1988; Greeley and Crown, 1990; Crown and Greeley, 1993). Detailed geologic study of the summit caldera and flanks of Hadriaca Patera is essential to determine the types of volcanic materials exposed, the nature of the processes forming these deposits, and the role of volcanism in the evolution of the cratered highlands that are characteristic of the southern hemisphere of Mars.

GENERAL GEOLOGY

The area east of Hellas Planitia is a complex geologic region affected by volcanism, tectonism, and channel- and canyon-forming processes (Crown and others, 1992; Tanaka and Leonard, 1995; Gregg and others, 1998; Price, 1998; Leonard and Tanaka, 2001; Mest and Crown, 2001; Crown and others, 2005b). The Hadriaca Patera summit region is dominated by the central caldera and eroded flanks of the volcano. North and west of its summit, Hadriaca Patera is bordered by older plateau and mountainous materials, including the rugged rim materials of Savich and Torup craters, Ausonia Montes, and Ausonia Mensa. The southeast flanks of Hadriaca Patera and the adjacent plains are cut by Dao and Niger Valles, which extend to the southwest into Hellas Planitia. The collapse depressions of Ausonia Cavus and Peraea Cavus define their uppermost extents. Plateau and mountainous materials to the north and east of Hadriaca Patera are embayed by an extensive flank flow unit that extends from the summit area of Tyrrhena Patera and contains numerous lava flow lobes. Many impact craters, such as Gander, Nazca, and Bazas on or adjacent to Hadriaca Patera and Savich and Torup to the northeast, are apparent throughout the map area; some exhibit smooth, flat floors indicating modification and infilling by sedimentary processes (Mest and Crown, 2005, 2006; Moore and Howard, 2005).

STRATIGRAPHY

We identified and mapped geologic units in MTM –30262 and –30267 quadrangles, based on analyses of morphologic characteristics in Viking Orbiter images. We determined stratigraphic positions, based on superposition, cross-cutting, and embayment relations, as well as crater size-frequency distributions. Geologic unit descriptions are based on photogeologic analyses of Viking Orbiter images and examination of recently acquired Mars Global Surveyor Mars Orbiter Camera (MOC) and Mars Odyssey Thermal Emission Imaging System (THEMIS) images.

The oldest units in the area are mountainous material (unit Nm) and the dissected unit of the plateau sequence (unit Npld; Greeley and Guest, 1987). Noachian mountainous material forms large, rugged blocks that rise above the surrounding plains, such as those exposed in Ausonia Montes and Ausonia Mensa. Other exposures of mountainous material appear to be remnants of large impact crater rims, such as Savich Crater. This material was uplifted and emplaced during an interval of intense cratering early in Martian history, and many exposures may have been associated with the formation of the impact basin that now contains Hellas Planitia. At the margins of many mountains, channels or gullies indicate modification by mass-wasting or fluvial processes. In MTM –30262 quadrangle, smooth material forms aprons of debris on the south side of Ausonia Mensa (fig. 4). These aprons are composed of talus material (unit At) shed from steep slopes and may be among the youngest landforms in the region. The Noachian dissected plateau unit (Npld), both in Ausonia Mensa and between Ausonia Montes and Torup crater, exhibits heavily cratered surfaces but contains some smooth areas and regions dissected by small channels and troughs approximately 0.5–2.5 km wide. This unit is typical of the cratered highlands of Mars and is found throughout the southern hemisphere.

The Hesperian smooth unit of the plateau sequence (unit Hpl$_3$) forms flat, relatively featureless plains filling low-lying areas adjacent to the older plateaus and mountainous regions and constitutes a widespread unit that typifies modification of the heavily cratered highlands (fig. 4; Greeley and Guest, 1987). Surface features include ridges and scarps. THEMIS images show that surface features mapped from Viking Orbiter images include ridges of apparent tectonic origin, erosional scarps, and margins of flow lobes that are similar to those mapped in the Tyrrhena Patera flank flow unit (AHtf). The smooth unit of the plateau sequence in the map area is composed of fluvial and aeolian sedimentary deposits and volcanic flows that fill the interior of Savich Crater and that are adjacent to Bazas and Torup craters, Ausonia Montes, Ausonia Mensa, Ausonia Cavus, and Peraea Cavus.

Hadriaca Patera flank materials, which surround the caldera, are divided into two units: Hadriaca Patera upper flank material (unit Hhfu) and Hadriaca Patera lower flank material (unit Hhfl). The upper flank material is proximal to Hadriaca Patera caldera-filling material (unit Hhc) and is bordered by scarps (fig. 3). Upper flank material forms a plateau that is relatively continuous to the north, extending more than 100 km from the caldera rim. Several layers are exposed northwest of the caldera in upper flank material, although the surface of upper flank material is generally smoother than that of lower flank material in Viking Orbiter images. South and west of the caldera, upper flank material consists of topographically high remnants that form the materials capping ridges within Hadriaca Patera lower flank material. Hadriaca Patera lower flank material consists of layered, dissected deposits underlying Hadriaca Patera upper flank material and surrounding Hadriaca Patera caldera-filling material. Numerous scarps define multiple layers within these deposits and bound the ridges between channels, which are oriented radially to the caldera (fig. 5). Isolated mesas that are also aligned in a radial pattern to the caldera are observed both adjacent to the caldera and farther down the flanks and indicate that the ridges are erosional remnants of the upper and lower flank materials (Crown and Greeley, 1993).

Hadriaca Patera, which has dimensions of approximately 300 by 560 km, is dominated by its channeled flanks, which are elongated to the southwest along the regional slope from Hesperia Planum to Hellas Planitia. Flank slopes estimated from Viking data range from approximately 0.09° in the north to approximately 0.47° in the west and south, where the spacing between channels is smaller and the number of exposed layers is greater than to the north (Crown and Greeley, 1993). Slopes derived from Mars Orbiter Laser Altimeter (MOLA) 128 pixels/degree, gridded data confirm the low slopes (<1°) for Hadriaca Patera's flanks and show that to the northwest the flanks actually slope upward slightly (~0.25°; fig. 3). Given the magnitude and extent of subsidence inferred around Dao and Niger Valles (Crown and others, 2004, 2005b), it is possible that Hadriaca Patera has subsided as well. The asymmetry of the flank slopes could be partly explained by increasing subsidence from the summit region to the south toward Dao Vallis. Within the north flanks of Hadriaca Patera, the observed scarps do not form a distinct radial pattern and only a few layers are evident within the units. The morphologic differences observed in the channeled flanks of Hadriaca Patera, as well as the differences between Hadriaca Patera upper flank material (unit Hhfu, most prevalent in the north) and Hadriaca Patera lower flank material (unit Hhfl), are attributed to changes in topography and the resulting changes in the degree of erosion, rather than to significant material differences as a consequence of changes in composition or emplacement style (Crown and Greeley, 1993).

The channels contained within the flanks of Hadriaca Patera are degraded, trough-shaped valleys that lack tributaries (Gulick and Baker, 1990; fig. 5). Theater heads are observed both adjacent to the caldera and on the southwest flanks. Many of the channels are continuous for long distances; however, some channels are discontinuous and others emanate from local topographic highs (crests of the ridges) on the flanks. Evidence for channel widening and the existence of theater heads indicates that groundwater sapping may have enlarged the channels (Gulick and Baker, 1990). On the southwest flanks, small V-shaped channels in the central parts of the larger troughs suggest dissection by surface runoff (Crown and Greeley, 1993). The morphology of the channels and related scarps and the presence of remnant mesas indicate that Hadriaca Patera exhibits an erosional surface morphology; the inferred friable nature of the materials within the flanks of Hadriaca Patera is also consistent with the volcano being composed of pyroclastic deposits (Crown and Greeley, 1993; Crown and others, 1992). No primary effusive volcanic features are evident on the flanks of Hadriaca Patera in Viking Orbiter images.

Analyses of MOC narrow-angle and THEMIS visible (VIS) and infrared (IR) images of the upper and lower flank materials of Hadriaca Patera support Viking-based interpretations of a dissected volcanic surface that lacks primary flow features. THEMIS images show that well-defined ejecta blankets associated with craters approximately 5–15 km in diameter superpose both the locally high standing flank materials (units Hhfu, Hhfl) and the floors of adjacent erosional valleys (Crown and others, 2005a; Williams and others, 2005). This suggests that both the formation and the main period of dissection of the flank materials were ancient, as constrained by crater counts from Viking Orbiter images (table 1). The limited dissection of some of these ejecta blankets by V-shaped inner channels in the wider radial valleys and the presence of fine-scale troughs perpendicular to radial valleys at the south margin of Hadriaca Patera suggest sustained or renewed erosion of the patera flanks, at least in some localities (Crown and others, 2005b).

The caldera-filling material (unit Hhc) at Hadriaca Patera exhibits smooth, relatively featureless surfaces (fig. 3). The caldera is approximately 77 km across. The caldera wall is well defined to the west, whereas a north or east caldera rim is not apparent, possibly due to either overflow or mantling by volcanic materials. The eastern caldera floor is topographically higher than the remainder of the caldera floor, and its surface exhibits many small (<2 km across), dome-like features that could be either erosional remnants of an ash deposit or lava flow or constructional volcanic landforms, such as lava domes or cones. In Viking Orbiter images, their origin is unclear; in MOC narrow-angle and THEMIS VIS images, many of these dome-like features appear buried or degraded, without clear preservation of their primary volcanic morphology. Scarps are evident within the caldera and extend into the surrounding flanks of the volcano. Although most of the scarps appear to be erosional, some may be degraded tectonic features, and a large scarp near the southwest margin of the caldera may be a flow margin of ponded lavas.

Based on morphological characteristics, the flanks of Hadriaca Patera consist of eroded pyroclastic deposits, with potential effusive activity subsequently producing caldera-filling deposits. Gravity-driven flow models demonstrate that the distribution of flank materials may be attributed to the emplacement of pyroclastic flows (Crown and Greeley, 1993). Layering, exposed within the flank materials by groundwater sapping and runoff, may be the result of different degrees of welding. From an energy perspective, both magmatic and hydromagmatic eruption models are viable (Crown and Greeley, 1993). Geomorphic analyses and mapping indicate an extended and complex history of volatile-driven activity in the region surrounding Hadriaca Patera (Crown and others, 1992; Mest and Crown, 2001; Crown and others, 2005b). The regional geologic setting and analyses of the potential supply of groundwater are consistent with hydrovolcanic activity (Crown and Greeley, 1993). Similarities in flank materials suggest that Tyrrhena and Hadriaca Paterae had comparable volcanic and erosional histories; however, Tyrrhena Patera exhibits evidence for greater structural modification at its summit than Hadriaca Patera and for extensive effusive activity on its southwest flank (Greeley and Crown, 1990). The V-shaped channels observed in the central parts of the larger valleys within Hadriaca Patera's flanks suggest a greater degree of runoff relative to Tyrrhena Patera, which is consistent with evidence for enhanced (and younger) volatile-driven activity in proximity to Hadriaca Patera (Crown and others, 2005b).

The eastern part of MTM –30262 quadrangle is dominated by a distinctive flank flow unit (unit AHtf) that extends from Tyrrhena Patera. This unit contains many flow lobes and leveed channels (fig. 4). Some of the channels are discontinuous and may represent partly collapsed lava tubes. The flow lobes within the flank flow unit are elongated to the southwest, and some are longer than 100 km. Morphologic similarities to terrestrial basaltic lava flows suggest similar eruptive conditions (Crown and others, 1991). The entire flank flow unit extends more than 1,000 km from the summit area of Tyrrhena Patera to the southwest. Near Hadriaca Patera, the flank flow unit embays the rugged massif of Ausonia Mensa (units Nm, Npld) and covers the smooth unit of the plateau sequence (unit Hpl$_3$). The flank flow unit merges with channeled plains east of Hellas Planitia, which is south of MTM –30262 quadrangle. The lava flows within this unit are definitive evidence for effusive volcanic deposits associated with the highland paterae (Greeley and Crown, 1990; also Moore and Thompson, 1991). Many ridges are observed within this unit, and some appear to have flows extending along or from them (Porter and others, 1991). Dominant ridge trends within the entire flank flow unit include orientations both radial and concentric to Hellas Planitia (Crown and others, 1992).

Many channels are evident within the geologic materials in MTM –30262 and –30267 quadrangles. Channels that are interpreted to be volcanic in origin are found within volcanic units, often in the centers of lava flow lobes. These channels appear to be high standing and constructional, rather than erosional. Typically, volcanic channels may also have segments that exhibit partial collapse of roof materials. Volcanic channels are differentiated from other channels on the map. Other channels in the region are attributed to fluvial and mass-wasting processes. Some channels represent fluvial activity, because they appear to be parts of larger drainage systems, dissect the local surface, and are sometimes directly associated with Dao or Niger Vallis. Evidence of fluvial deposition or of features specifically diagnostic of fluvial erosion is not observed in Viking Orbiter images. Analyses of MOC images of parts of Dao and Niger Vallis show that lineations interpreted to be scour marks due to fluvial erosion in Viking Orbiter images are actually the result of collapse and breakdown of plains materials (Crown and others, 2004).

The east and southeast flanks of Hadriaca Patera and the west margin of the flank flow unit are dissected by the Dao and Niger Valles canyon systems. Dao and Niger Valles are parallel canyon systems that merge south of Hadriaca Patera and may have both surface and subsurface connections along east and southeast margins of Hadriaca Patera. Vallis floor material (unit AHv) is observed in two smooth-floored, steep-walled depressions (Peraea Cavus and Ausonia Cavus) that represent the upper reaches of the canyon systems. Small knobs on their floors may be remnants of collapsed plains or accumulations of sedimentary material. In Viking Orbiter images, no layering in canyon walls or interior layered deposits are observed. MOLA topographic profiles show that the depressions are a kilometer or more deep and deepen toward their centers (Crown and Mest, 2001). MOC images show that the floors of the depressions exhibit smooth, knobby, and hummocky surfaces. Dune forms are present and are concentrated in local low-lying regions, and the upper parts of the walls are layered. In Ausonia Cavus, small layered and rounded hills are presumably slump blocks of surrounding plains material.

Peraea Cavus and Ausonia Cavus are separated from the main canyons of Dao and Niger Valles (south of map area) by zones of collapsed and subsided plains (Squyres and others, 1987; Crown and others, 1992; Mest and Crown, 2001; Crown and others, 2004). These materials are mapped as irregular vallis floor material (unit AHvi), which exhibits surfaces dissected by small channels and troughs. We interpret irregular vallis floor material as volcanic flank materials and smooth plateau material that have undergone the initial stages of dissection and collapse. Parts of their surfaces clearly exhibit characteristics of the surrounding plains, whereas other areas of plains material appear to have been significantly altered by some combination of collapse, erosion, and deposition. MOLA topographic data show subsided plains as much as 500 m below surrounding materials, although the magnitude of subsidence is typically less and shows a high degree of spatial variability (Crown and others, 2004).

Vallis floor material (unit AHv) denotes regions where pre-existing materials were almost completely removed by a combination of surface and subsurface flow (Squyres and others, 1987; Crown and others, 1992). The canyon floor in these areas is presumably depositional. While the relative ages between the valles materials are poorly constrained, the incomplete dissection of the irregular vallis floor material suggests that it is older than the vallis floor material. Evidence for subsurface flow and collapse in association with Dao and Niger Valles suggests that the near-surface materials in this region are water or ice rich (Crown and others, 2004, 2005b).

Craters and their associated rim and ejecta materials are divided into three classifications based upon their state of degradation and stratigraphic relations: (1) well-preserved crater material (unit c$_3$) exhibits pronounced, continuous crater rims, steep inner walls, and generally well defined, continuous ejecta deposits; (2) moderately-degraded crater material (unit c$_2$) displays partially eroded rims and may have only poorly exposed, discontinuous ejecta deposits; and (3) highly degraded crater material has subdued and (or) discontinuous rims and generally has no recognizable ejecta deposits. Only craters with rim-crest diameters greater or less than 3 km are mapped. For each classification, crater rim material and crater ejecta material are mapped where possible. The blocky, rugged material forming the inner and outer rims of impact craters is designated crater rim material (units cr$_1$, cr$_2$, cr$_3$), and the rough-textured deposits surrounding crater rims and subduing or mantling the underlying topography are crater ejecta material (units ce$_2$, ce$_3$). Some crater ejecta deposits have bounding scarps and appear to have been emplaced as fluid flows. Ejecta from the crater Isil embays plateau and mountain material and the northwestern margin of Hadriaca Patera in the northwest corner of MTM –30267. This ejecta blanket is mapped as unit ce$_2$; whereas, Mest and Crown (2006) map Isil ejecta as unit c$_3$ based on the presence of discrete ejecta flow lobes observed adjacent to the crater rim (outside the map area). In Viking Orbiter images, crater floor material (unit cf) consists of smooth deposits filling craters and may contain some scarps and channels. Crater floor material may have diverse origins, and we interpret it as sedimentary deposits, most likely emplaced by mass-wasting or aeolian processes; contributions of glacial, fluvial, and lacustrine sediments are also possible. Crater floor material may be similar in age to or significantly younger than the formation of the crater in which it is found. Crater central peaks, mapped as crater floor material, consist of knobby or hilly materials found on crater floors. A central peak is observed in Gander crater (~35 km diam) southeast of the Hadriaca Patera caldera.

GEOLOGIC HISTORY

The geologic history of the Hadriaca Patera summit region is derived primarily from analysis of Viking Orbiter images and supplemental information from MOLA topographic data and MOC and THEMIS images. The evolution of the region and the relative ages of the units are supported by crater size-frequency distributions presented in the regional study of Crown and others (1992; table 1). The observed types of geologic materials, the geomorphologic characteristics of the units, and the apparent stratigraphic relations suggest the following sequence of events in order of occurrence:

1. Uplift of Noachian mountains and plateau materials (units Nm, Npld) in association with and following the impact event centered in the location of Hellas Planitia. Materials are preserved as isolated massifs and heavily cratered terrain that contain remnants of large crater rims (unit cr$_1$).
2. Dissection of the Noachian upland materials and emplacement of Hesperian smooth unit of the plateau sequence (unit Hpl$_3$), involving sedimentary and volcanic processes.
3. Formation of Hadriaca Patera, including the central caldera. Flank materials (units Hhfu, Hhfl) are interpreted as pyroclastic deposits, presumably emplaced as flows. Both explosive and effusive eruptive activity may have contributed to formation of the caldera deposits (unit Hhc).
4. Erosion of the flanks of Hadriaca Patera, presumably by groundwater sapping and localized surface runoff along the south flanks of the volcano.
5. Emplacement of the lava flows and lava channels from Tyrrhena Patera (unit AHtf). Ridges formed by compression after and, possibly, during flow emplacement; some ridges may be partially volcanic and delineate source vents for lava flows. Contractional deformation also affects Hadriaca Patera flank materials (units Hhfu, Hhfl) and the smooth unit of the plateau sequence (unit Hpl$_3$).
6. Formation of Dao and Niger Valles. Fluvial activity may include groundwater sapping, subsurface flow, and local surface runoff. Collapse and removal of material is indicated by the morphology of vallis floor materials (units AHv, AHvi); Peraea and Ausonia Cavi provide evidence for formation of discrete collapse features at upper extents of Dao and Niger Valles, with subsurface connections to the main parts of the canyon systems.
7. Talus deposits (unit At) shed from the steep south side of Ausonia Mensa.
8. Impact events that produce crater materials (units c$_2$, c$_3$; ejecta and rim subunits) during and subsequent to the previous events. Sediment accumulates on the floors of some craters (unit cf) due to a variety of degradational processes.

ACKNOWLEDGMENTS

This research was supported by the NASA Planetary Geology and Geophysics Program. Helpful reviews were provided by Ted Maxwell and Jim Zimbelman. We thank Les Bleamaster for assistance with figure preparation. MOC images courtesy of National Aeronautics and Space Administration (NASA), Jet Propulsion Laboratory (JPL), and Malin Space Science Systems. THEMIS images courtesy of NASA, JPL, and Arizona State University. MOLA data courtesy of NASA Goddard Space Flight Center.

REFERENCES CITED

Crown, D.A., Berman, D.C., Bleamaster, L.F., Chuang, F.C., and Hartmann, W.K., 2005a, Martian highland paterae—Studies of volcanic and degradation histories from high-resolution images and impact crater populations [abs.]: Houston, Tex., Lunar and Planetary Institute, Lunar and Planetary Science Conference, XXXVI, Abstract no. 1476 [CD-ROM].

Crown, D.A., Bleamaster, L.F., and Mest, S.C., 2004, Geologic evolution of Dao Vallis, Mars [abs.]: Houston, Tex., Lunar and Planetary Institute, Lunar and Planetary Science Conference, XXXV, Abstract no. 1185 [CD-ROM].

Crown, D.A., Bleamaster, L.F., and Mest, S.C., 2005b, Styles and timing of volatile-driven activity in the eastern Hellas region of Mars: Journal of Geophysical Research, v. 110, E12S22 (doi:10.1029/2005JE002496).

Crown, D.A., and Greeley, Ronald, 1993, Volcanic geology of Hadriaca Patera and the eastern Hellas region of Mars: Journal of Geophysical Research, v. 98, p. 3431–3451.

Crown, D.A., Greeley, R., and Sheridan, M.F., 1988, Consideration of hydromagmatic origins for Hadriaca Patera and Tyrrhena Patera [abs.]: Houston, Tex., Lunar and Planetary Institute, Lunar and Planetary Science Conference, XIX, p. 229–230.

Crown, D.A., and Mest, S.C., 2001, Circum-Hellas outflow channels—New views from Mars Global Surveyor [abs.]: Houston, Tex., Lunar and Planetary Institute, Lunar and Planetary Science Conference, XXXV, Abstract no. 1344 [CD-ROM].

Crown, D.A., Porter, T.K., and Greeley, R., 1991, Physical properties of lava flows on the southwest flank of Tyrrhena Patera, Mars [abs.]: Houston, Tex., Lunar and Planetary Institute, Lunar and Planetary Science Conference, XXII, p. 261–262.

Crown, D.A., Price, K.H., and Greeley, R., 1992, Geologic evolution of the east rim of the Hellas basin, Mars: Icarus, v. 100, p. 1–25.

Francis, P.W., and Wood, C.A., 1982, Absence of silicic volcanism on Mars—Implications for crustal composition and volatile abundance: Journal of Geophysical Research, v. 87, p. 9881–9889.

Greeley, R., and Crown, D.A., 1990, Volcanic geology of Tyrrhena Patera, Mars: Journal of Geophysical Research, v. 95, p. 7133–7149.

Greeley, R., and Guest, J.E., 1987, Geologic map of the eastern equatorial region of Mars: U.S. Geological Survey Miscellaneous Investigations Series Map I–1802B, scale 1:15,000,000.

Greeley, R., and Spudis, P.D., 1981, Volcanism on Mars: Reviews of Geophysics and Space Physics, v. 19, p. 13–41.

Gregg, T.K.P., Crown, D.A., and Greeley, Ronald, 1998, Geologic map of MTM quadrangle –20252, Tyrrhena Patera region of Mars: U.S. Geological Survey Miscellaneous Investigations Series I–2556, scale 1:500,000.

Gulick, V.C., and Baker, V.R., 1990, Origin and evolution of valleys on Martian volcanoes: Journal of Geophysical Research, v. 95, p. 14,325–14,344.

King, E.A., 1978, Geologic map of the Mare Tyrrhena quadrangle of Mars: U.S. Geological Survey Miscellaneous Investigations Series Map I–1073, scale 1:5,000,000.

Leonard, G.J., and Tanaka, K.L., 2001, Geologic map of the Hellas Region of Mars: U.S. Geological Survey Geologic Investigations Series I–2694, scale 1:4,336,000.

Mest, S.C., and Crown, D.A., 2001, Geologic history of the Reull Vallis Region of Mars: Icarus, v. 153, p. 89–110.

Mest, S.C., and Crown, D.A., 2005, Millochau crater, Mars—Infilling and erosion of an ancient highland impact crater: Icarus, v. 175, no. 2, p. 335–359.

Mest, S.C., and Crown, D.A., 2006, Geologic map of MTM –20272 and –25272 quadrangles, Tyrrhena Terra region of Mars: U.S. Geological Survey Scientific Investigations Map 2934, 1:5,000,000.

Moore, J.M., and Howard, A.D., 2005, Large alluvial fans on Mars: Journal of Geophysical Research, v. 110, E04005 (doi:10.1029/2004JE002352).

Moore, H.J., and Thompson, T.W., 1991, A radar-echo model for Mars: Houston, Tex., Lunar and Planetary Institute, Proceedings of Lunar and Planetary Science, v. 21, p. 457–472.

Peterson, J.E., 1977, Geologic map of the Noachis quadrangle of Mars: U.S. Geological Survey Miscellaneous Investigations Series Map I–910, scale 1:5,000,000.

Peterson, J.E., 1978, Volcanism in the Noachis-Hellas region of Mars, 2, *in* Proceedings of the Lunar and Planetary Science Conference, 9th: New York, Pergamon Press, Geochimica Et Cosmochimica Acta, Supplement 11, p. 3411–3432.

Plescia, J.B., and Saunders, R.S., 1979, The chronology of the Martian volcanoes, *in* Proceedings of the Lunar and Planetary Science Conference, 10th: New York, Pergamon Press, Geochimica Et Cosmochimica Acta, Supplement 10, p. 2841–2859.

Porter, T.K., Crown, D.A., and Greeley, R., 1991, Timing and formation of wrinkle ridges in the Tyrrhena Patera region of Mars [abs.]: Houston, Tex., Lunar and Planetary Institute, Lunar and Planetary Science Conference, XXII, p. 1085–1086.

Potter, D.B., 1976, Geologic map of the Hellas quadrangle of Mars: U.S. Geological Survey Miscellaneous Investigations Series Map I–941, scale 1:5,000,000.

Price, K.H., 1998, Geologic map of MTM quadrangles –40262, –40267, and –40272: Dao, Harmakhis, and Reull Vallis regions of Mars: U.S. Geological Survey Miscellaneous Investigations Series I–2557, scale 1:500,000.

Schultz, P.H., 1984, Impact basin control of volcanic and tectonic provinces on Mars [abs.]: Houston, Tex., Lunar and Planetary Institute, Lunar and Planetary Science Conference, XV, p. 728–729.

Scott, D.H., and Carr, M.H., 1978, Geologic map of Mars: U.S. Geological Survey Miscellaneous Investigations Series Map I–1083, scale 1:25,000,000.

Squyres, S.W., Wilhelms, D.E., and Moosman, A.C., 1987, Large-scale volcano-ground ice interactions on Mars: Icarus, v. 70, p. 385–408.

Tanaka, K.L., 1986, The stratigraphy of Mars, *in* Proceedings of the Lunar and Planetary Science Conference, 17th, Part 1: Journal of Geophysical Research, v. 91, supplement, p. E139–E158.

Tanaka, K.L., and Leonard, G.J., 1995, Geology and landscape evolution of the Hellas region of Mars: Journal of Geophysical Research, v. 100, p. 5407–5432.

Williams, D.A., Greeley, R., Zuschneid, W., Werner, S., Neukum, G., Crown, D.A., Gregg, T.K.P., Raitala, J., and the HRSC Co-Investigator Team, 2005, Hadriaca Patera—Volcanic history derived from HRSC-based crater counts [abs.]: Houston, Tex., Lunar and Planetary Institute, Lunar and Planetary Science Conference, XXXVI, Abstract no. 1470 [CD-ROM].

Geologic Map of MTM –30262 and –30267 Quadrangles, Hadriaca Patera Region of Mars

By
David A. Crown[1] and Ronald Greeley[2]
2007

[1]Planetary Science Institute, Tucson, AZ
[2]School of Earth and Space Exploration, Arizona State University, Tempe, AZ

ISBN 1-411-31762-9
9 781411 317628

Any use of trade, product, or firm names in this publication is for descriptive purposes only and does not imply endorsement by the U.S. Government
For sale by U.S. Geological Survey, Information Services, Box 25286, Federal Center, Denver, CO 80225, 1-888-ASK-USGS
Available at http://pubs.usgs.gov/sim/2007/2936
Printed on recycled paper